Chemical Methodologies 6(2022) 372-384

Chemical Methodologies

Journal homepage: http://chemmethod.com

Original Research Article

Synthesis of New Schiff Base from Antibiotics and Some of Its Metal Complexes with Study Some of Their Applications

Amna Ahmed Neamah*, Asmaa Mohammed Noori Khaleel

Department of Chemistry, College of Science, University of Baghdad, Iraq

ARTICLE INFO

Article history

Submitted: 2022-03-08
Revised: 2022-03-16
Accepted: 2022-03-25
Manuscript ID: CHEMM-2203-1451
Checked for Plagiarism: **Yes**
Language Editor:
Dr. Fatimah Ramezani
Editor who approved publication:
Professor Dr. Lotfali Saghatforoush

DOI:10.22034/CHEMM.2022.333061.1451

KEYWORDS

Schiff base
Sulfamethoxazole
Tenoxicam

ABSTRACT

Synthesis of new Schiff base ligand (L) from sulfamethoxazole with tenoxicam in mole ratio 1:1. The metal complexes were synthesized by the reaction of ($CoCl_2.6H_2O$, $NiCl_2.6H_2O$ $CuCl_2.2H_2O$) with Ligand in mole ratio 2:1 (L:M). The characterization of all synthesized compounds carried out by spectral methods such as ultra violet and visible radiation (UV-Vis), infrared (FT-IR), nuclear magnetic resonance of protons (^{1}H-NMR), thermal analyses (TG, DTG) and atomic absorption (AAS) as well as melting point (m.p) measurement, micro elemental analysis (CHNS), magnetic susceptibility measurement and determination of chloride content. The suggested geometries of all complexes were octahedral. All complexes were electrolyte and paramagnetic. All of the synthesized compounds were found to be anti-bacterial and anti-fungal against bacteria Klebsiella pneumonia (G-) and Staphylococcus aurus (G+) as well as fungi rizopussporium. Also anti-cancer property of the ligand was tested.

GRAPHICAL ABSTRACT

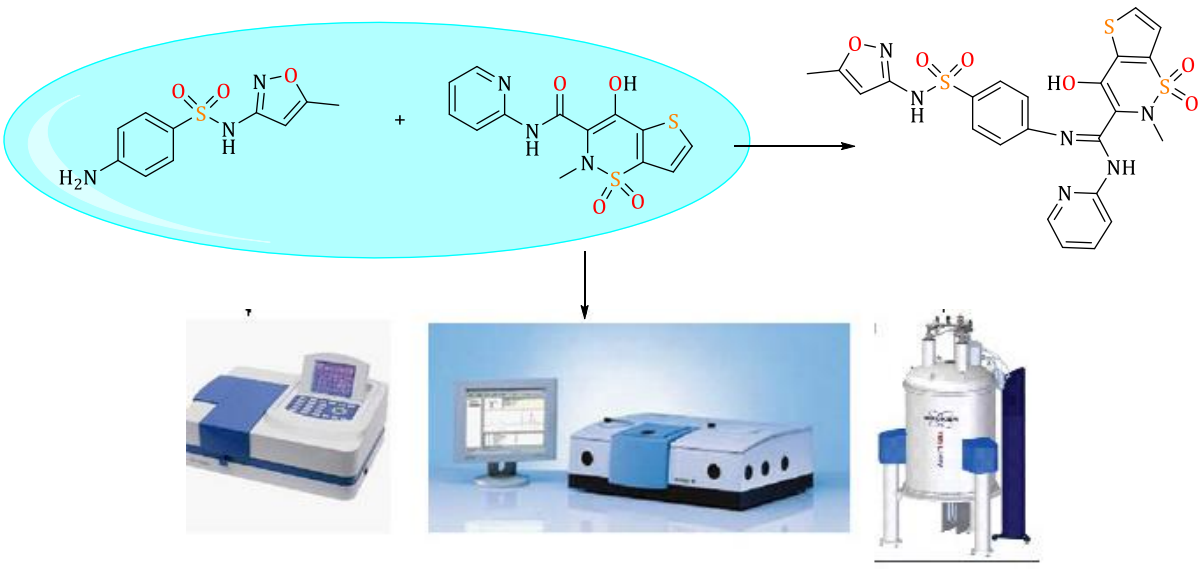

* Corresponding author: Amna Ahmed Neamah,
✉ E-mail: amnajuda97@gmail.com

Introduction

Antibiotics are substances which kill bacteria without harming the host, or human. Antibiotic means "against" and "biotic" means "life-giving" [1]. Antibiotics are either natural substances produced in nature by microorganisms or synthetic substances created in a laboratory. To be considered a clinically effective antibiotic and thus useful in medicine, the microorganism should be destroyed or inhibited in the respective concentrations of the antibiotic in the body [2]. Antibiotics with a broad spectrum of action, such as penicillin, kill many different types of bacteria. Broad spectrum antibiotics are effective against a wide range of microbes, including bacteria, rickettsia, mycoplasmas, protozoa, and spirochetes. Narrow-spectrum antibiotics, such as isoniazid, kill specific types of bacteria and should be used whenever possible to reduce the risk of resistant bacteria *colonization* and *superinfection* [3].

Sulfamethoxazole (SMX) is a sulfonamide antibiotic which has been widely used in the treatment of bacterial infections in humans, such as urinary tract infections, bronchitis, and prostatitis. SMX is effective against both gram-negative and gram-positive bacteria and is widely used in the animal husbandry and aquaculture industries for the treatment of bacterial infections. Sulfanilamide sulfamethoxazole is a structural analog of para-aminobenzoic acid (PABA). The mechanism of action is to inhibit dihydropteroic acid formation by inhibiting dihydropteroate synthase, thereby inhibiting bacterial growth [4,5].

Tenoxicam is a new nonsteroidal anti-inflammatory drug used to treat musculoskeletal and joint disorders like osteoarthritis of the knee and acute gout [6,7]. Tenoxicam contains a five-membered heteroatom ring that is responsible for the drug's clinical activity. Tenoxicam behaves as a bidentate ligand when it is coordinated with metal ions via the pyridyl ring amide oxygen and nitrogen atoms [8].

In this study, we are synthesizing the Schiff base ligand from the reaction of sulfamethoxazole with tenoxicam and evaluating its anti-microbial and anti-cancer activity. In addition, we are synthesizing metal complexes of this Schiff base ligand with Co (II), Ni (II), and Cu (II) metal ions to investigate their effect on biological activity. All synthesized compounds were tested as anti-microbial and the ligand was tested as anti-cancer.

Materials and methods

Elemental microanalyses (CHNS) for carbon, hydrogen, nitrogen, and sulfur were recorded by the elemental analyzer EuroEA 3000/Italy. The melting points were determined using the Gallenkamp melting point apparatus. The FTIR (Fourier Transform Infra-Red) spectrophotometry for the ligands in the range 400 – 4000 cm^{-1} (KBr) and for the complexes in the range 250 – 4000 cm^{-1} (CsI). UV-Visible spectra were measured using a (Shiamadzu 1800-UV spectrophotometer) in range (240 -1100) nm with DMSO as a solvent. NMR Bruker 500MHz Germany measured ^1H -NMR spectra in DMSO-d_6. Thermal analyses (TG, DTG) were documented (Tga dta sta300 Germany). Sherwood Scientific's Auto Magnetic Susceptibility Balance Model was used to record magnetic susceptibility measurements at ambient temperature. On a Nova350 Spectrophotometer, the metal content was determined using atomic absorption spectroscopy. The Mohr method was used to determine the chloride content of complexes. Agar diffusion was used to test antibacterial activity.

Synthesis of the ligand 4_hydroxy-2-methyl-N-(4-(N-(5-methylisoxal-3-yl)sulfamyl)phenyl)-N-(pyridin-2-yl)-3,4-dihydro-2H-thieno[2,3-e][1,2]thiazine-3-carboximidamide1,1-dioxide (L)

Tenoxicam (0.1332 g, 0.394 mmol) in 40 mL ethanol was heated under reflux for 20 minutes with stirring until complete solubility, then Sulfamethoxazole (0.1 g, 0.394 mmol) in 5 mL ethanol was heated under reflux with stirring, two drops of glacial acetic acid were added, and the reaction was continued. The reaction was terminated after the solution was tested using TLC, which took a total of 10 hours. After heating the solution to evaporate some of the solvent, the yellow product was obtained by cooling in an ice bath and scratching, washing with ethanol and

drying in an oven at 80 degrees Celsius. The first Scheme is as follows:

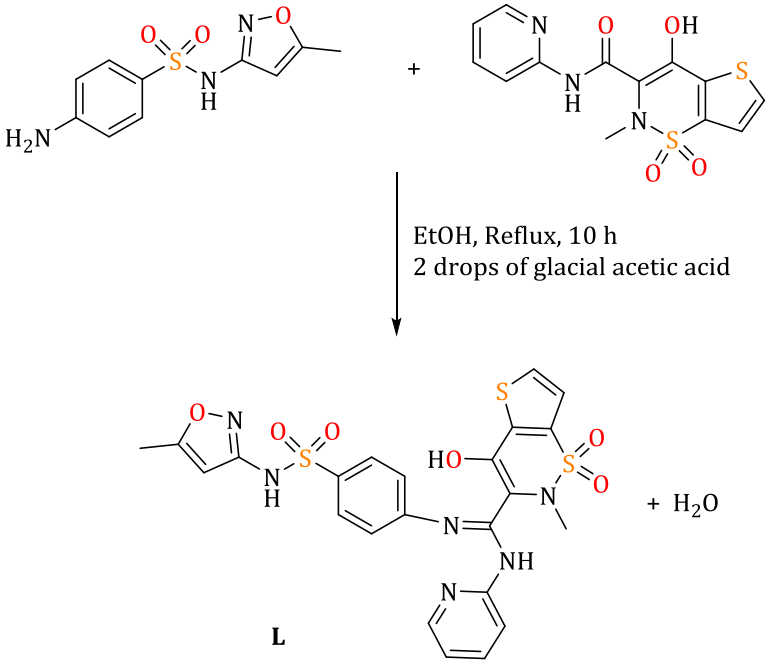

Scheme 1: Schiff base ligand structure

Synthesis of L complex with Co (II) (C_1)

C1 complex synthesis at a mole ratio of 2:1 (L:M). The solution of L (0.1 g, 0.174 mmol) in 25mL ethanol (yellow) was heated under reflux for 20 minutes with stirring until complete solubility, and then the metal salt $CoCl_2.6H_2O$ (0.020 g, 0.084 mmol) was added to 5 mL ethanol (blue), a yellowish green color appeared immediately and the solution was heated under reflux for 5 hours with stirring. The solvent was evaporated, revealing the greenish yellow product, which was then cooled in an ice bath and scratched before being washed with hot ethanol and dried in an oven at 80 °C.

Synthesis of L complex with Ni (II) (C2)

The solution of L (0.1 g, 0.174 mmol) in 20 mL ethanol (yellow) was heated under reflux for 20 minutes with stirring until complete solubility, and then the metal salt $NiCl_2.6H_2O$ (0.020 g, 0.084 mmol) appeared immediately in 5 mL ethanol (phosphorous green) and the solution was heated under reflux for 5 hours with stirring. The solvent was evaporated, resulting in a yellowish green product which was scratched and cooled in an ice bath before being washed with hot ethanol and dried in an oven at 80 °C.

Synthesis of L complex with Cu (II) (C3)

The solution of L (0.1 g, 0.174 mmol) in 25 mL ethanol (yellow) was heated under reflux for 20 minutes with stirring until complete solubility, and then the metal salt $CuCl_2.2H_2O$ (0.015 g, 0.087 mmol) was added to 5 mL ethanol (phosphorescent green), reddish orange color was immediately appeared and the solution was heated under reflux for 5 hours with stirring, after 15 minutes the color was the solvent was evaporated, revealing a dark green product which was scratched, washed with hot ethanol and dried in an oven at 80 °C.

Biological Evaluation (Anti-microbial activity)

The anti-bacterial and anti-fungal activities of all synthesized compounds were achieved by the well diffusion method using 10^{-3} M in DMSO solutions against *Klebsiella pneumonia(G-), Staphylococcus aurus (G+), and rizopussporium.* The inhibition diameters were measured in order to assess anti-microbial activity.

Results and Discussion

The physical properties, elemental analysis, metal content, and chloride content data illustrated in Table 1.

Table 1: Analysis data and Physical properties of the ligand and its metal complexes

Compund	The molecular formula	Color	m.p (°C)	Yield %	M.wt (g.mol^{-1})	Micro Elementa Analysis Found (Calc.)				Metal content %	Chloride content %
						C%	H%	N%	S%		
L_1	$C_{23}H_{20}N_6O_6S_3$	Dark yellow	180-182	90%	572	48.29 (47.22)	3.94 (3.12)	14.69 (13.56)	16.81 (16.05)	-----	-----
C1	$C_{46}H_{40}N_{12}O_{12}S_6CoCl_2.6H_2O$	Greenish yellow	230-232	85%	1381	39.97 (39.39)	3.76 (2.98)	12.16 (11.12)	13.90 (13.10)	5.14 (5.0)	4.26 (3.44)
C2	$C_{46}H_{40}N_{12}O_{12}S_6NiCl_2.6H_2O$	Yellowish green	250-252	82%	1381.6	37.78 (37.28)	3.76 (3.37)	12.15 (11.18)	13.89 (12.95)	5.13 (4.27)	4.24 (3.38)
C3	$C_{46}H_{40}N_{12}O_{12}S_6CuCl_2.6H_2O$	Dark green	118-120	89%	1386.5	39.81 (39.63)	3.75 (3.17)	12.11 (11.36)	13.84 (13.32)	5.12 (4.32)	4.54 (3.44)

Table 2: The name and molecular formula for the ligand (L) and its metal ion complexes

Compund	Formal	**N**ame
L	$C_{23}H_20N_6O_6S_3$	4-hydroxy-2-methyl-*N*-(4-(*N*-(5-methylisoxal-3-yl)sulfamyl)phenyl)-*N*-(pyridin-2-yl)-3,4-dihydro-2*H*-thieno[2,3-e][1,2]thiazine-3-carboximidamide1,1-dioxide
C_1	$[(L_1)_2CoCl_2].6H_2O$	Di chloro[bis{4-hydroxy-2-methyl-*N*'-(4-(*N*-(5-methylisoxazol-3-yl)sulfamoyl)phenyl)-*N*-(pyridin-2-yl)-2*H*-thieno[2,3-e][1,2]thiazine-3-carboximidamide 1,1-dioxide} cobalt (II)] 6 hydrate
C_2	$[(L_1)_2NiCl_2].6H_2O$	Di chloro[bis {4-hydroxy-2-methyl-*N*'-(4-(*N*-(5-methylisoxazol-3-yl)sulfamoyl)phenyl)-*N*-(pyridin-2-yl)-2*H*-thieno[2,3-e][1,2]thiazine-3-carboximidamide 1,1-dioxide} Nickel (II)] 6 hydrate
C_3	$[(L_1)_2CuCl_2].6H_2O$	Di chloro[bis {4-hydroxy-2-methyl-*N*'-(4-(*N*-(5-methylisoxazol-3-yl)sulfamoyl)phenyl)-*N*-(pyridin-2-yl)-2*H*-thieno[2,3-e][1,2]thiazine-3-carboximidamide 1,1-dioxide copper (II)] 6 hydrate

FTIR Spectroscopy

The FTIR spectra of cobalt, nickel, and copper complexes revealed shifting in the stretching vibration of the (OH group) (Table 3), owing to ligand coordination with metal ions via the OH group [9]. Stretching bands of NH_2 and amide carbonyl group were absent and appeared new band at 1637 cm^{-1} at lower frequency in complexes spectra attributed to coordination with metal ions [10,11]. Finally new stretching was appeared at lower frequencies which were assigned to (M-N), (M-O) [12].

Table 3: The Ligand's and its metal complex's characteristic infrared absorption bands

compund	υ(lattice H_2O) coord.H_2O	υ NH_2	υ OH	υ NH sulfon	υ NH amide	υ C=N	υ C=N cyclic	υ SO_2	υ M-N	υ M-O
Sulf	--	3379, 3467	--	3299	--	--	1596	1309	--	--
Teno	--	--	3437	--	3093	--	--	--	--	--
L_1	--	--	3434	3298	3091	1637	1598	1299	--	--
L_1Co	(3122),927	--	3456	3303	3093	1616	1596	1292	547	432
L_1Ni	(3134),921	--	3388	3301	3093	1616	1595	1294	547	453
L_1Cu	(3122),918	--	3458	3305	3097	1620	1598	1298	530	430

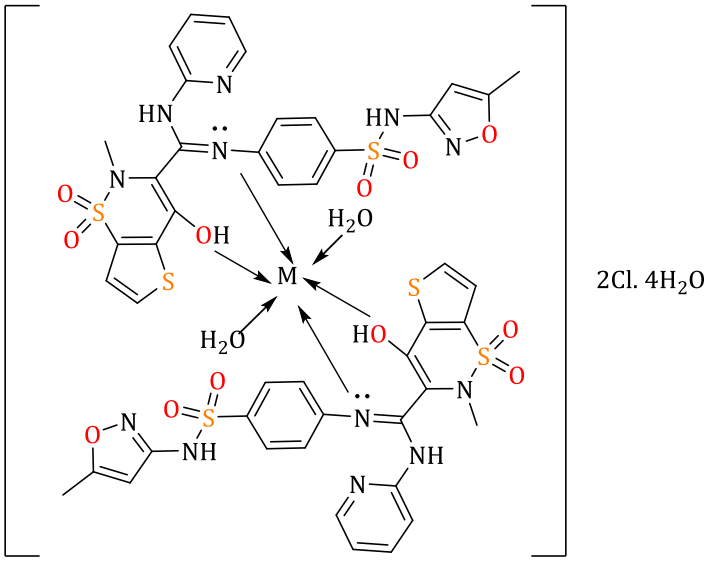

M=Co(II), Ni(II), Cu(II)

Scheme 2: The proposed structure of complexes

^{1}H-NMR Spectroscopy

The ligand (L) and its metal complexes were characterized by using ^{1}H-NMR in DMSO-d_6. The ^{1}H-NMR spectrum of the ligand was complexes revealed characteristic peaks of pyridine proton, OH proton, isoxazole ring, benzene proton, and sec-amide protons, all of which were consistent with previous studies [13-19]. The ligand's ^{1}H-NMR spectrum is displayed in (Scheme 3, Figure 1) and the ^{1}H-NMR data is indicated in Table 4.

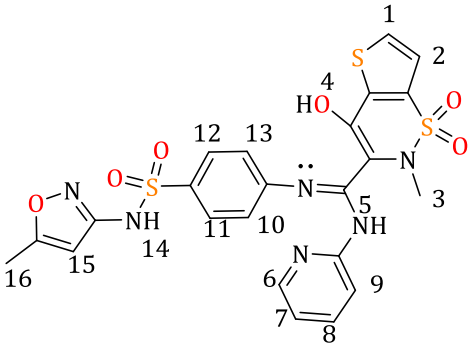

Scheme **3:** propose Structure of the ligand (L)

Table 4: ^{1}H-NMR data for the ligand (L)

Assignments in DMSO-d_6	Mark	Chemical shifts δ (ppm)
CH_3-methyl group	16	(2.13-2.45),3H,s
CH_3-methyl group	3	(2.67-2.93),3H,s
CH-isoxazole	15	(6.10-6.33),H,s
CH-Benzeze	11,12	(6.57-6.98),2H,t
CH-pyridine	8	(7.09-7.29),H,t
CH-pyridine	6	(7.31-7.34),H,d
CH-thiophene	2	(7.44-7.46),H,d
CH-Benzene	13,10	(7.48–7.60),2H,t
CH-pyridine	7	(7.72-7.74),H,t
CH-thiophene	1	(7.93-7.95),H,d
CH-pyridine	9	(8.01-8.27),H,d
NH-sec amide	5	(8.32-8.33),H,s
NH-sulfonamide	14	(10.95),H,s
OH -enol	4	(13.79),H,s

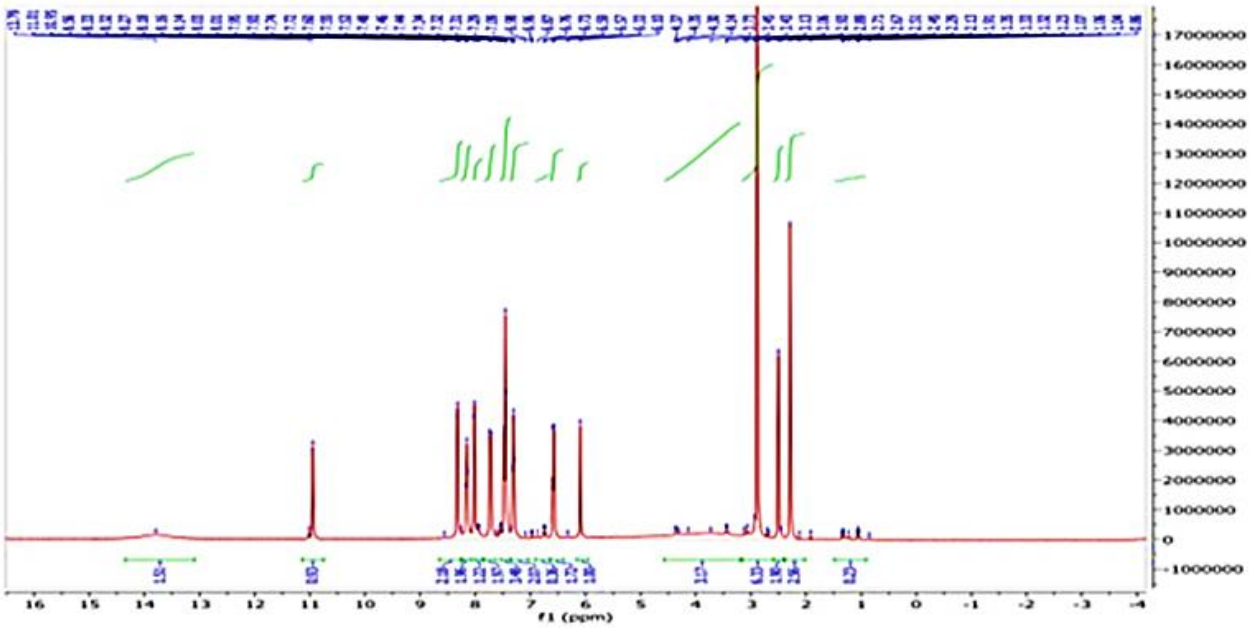

Figure 1: ^{1}H-NMR spectrum for the ligand

Thermal characterization of the ligand and its complexes:

TG (thermo-gravimetric) and DTG (differential thermo-gravimetric) data were analyzed with argon gas at temperatures ranging from 0 to 1000 °C (10 °C /min). This technique is used to obtain information about the thermal stability of synthesized compounds, as well as the nature of intermediate and final products. Figure 2 displays thermogram of the ligand.

Table 5: Thermal decomposition data for the ligand and its metal complexes

Compund	Molecular formula and molecular weight	Steps	TG temperature range ℃	DTG temp℃	Suggested formula of loss	Mass loss cal (found)
L	$C_{23}H_{20}N_6O_6S_3$ 572 g/mol	1	0-280 ℃	180,240℃	$C_{10}H_{13}N_3O_4$	41.78 (42.07)
		2	280-850 ℃	550℃	$C_6H_5N_2SO_2$	29.54 (29.53)
		residue	900 ℃	___	$C_7H_2NS_2$	28.67 (28.43)
C_1	$C_{46}H_{40}N_{12}O_{12}S_6CoCl_2.6H_2O$ 1381 g/mol	1	0-336 ℃	140,250,290 ℃	$C_{10}H_{29}N_3SO_{12}Cl_2$	35.19 (35.98)
		2	336-850 ℃	360 ℃	$C_{12}H_4N_2S_4O_4$	26.64 (26.36)
		residue	900 ℃	___	$C_{24}H_{19}N_7SO_2Co$	38.16 (37.96)
C_2	$C_{46}H_{40}N_{12}O_{12}S_6NiCl_2.6H_2O$ 1381.6 g/mol	1	0-298℃	110,190 ℃	$C_{10}H_{28}N_2O_{12}Cl_2$	31.77 (31.79)
		2	298-850℃	415,680℃	$C_{17}H_{10}N_5S_5O_4$	36.76 (36.90)
		residue	900℃	___	$C_{19}H_{14}N_5SO_2Ni$	31.45 (31.32)
C_3	$C_{46}H_{40}N_{12}O_{12}S_6CuCl_2.6H_2O$ 1386.5 g/mol	1	0-278℃	80, 190℃	$C_{10}H_{28}N_2O_{12}Cl_2$	31.66 (30.66)
		2	278-850 ℃	760℃	$C_{17}H_9N_4S_4O_4$	33.24 (33.20)
		residue	900℃	___	$C_{19}H_{15}N_6S_2O_2Cu$	35.08 (36.11)

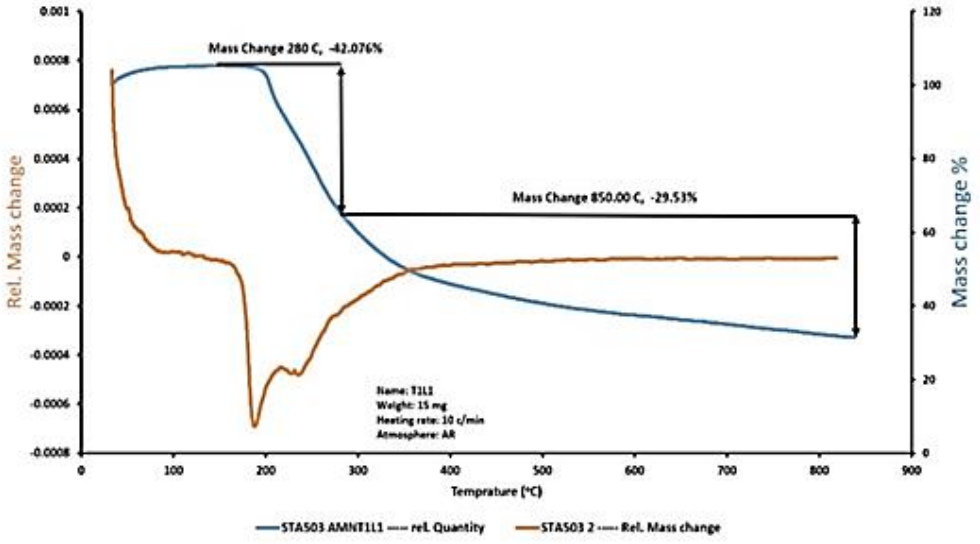

Figure 2: The thermogram of the ligand

Electronic Spectra

The electronic spectra of synthesized compounds were monitored in DMSO (10^{-3} M) at room temperature.

Electronic spectra of ligand

The ligand's electronic spectrum revealed two bands which were ascribed to the π-π* transition [20] at [382 nm (26178 cm^{-1}) and [271 nm (36900

cm^{-1}). Figure 3 depicts the ligand spectra, and the data are listed in Table 6.

Electronic spectra of cobalt (II) complexe (C_1)

The spectrum of the complex (C1) is illustrated in Figure 4 and the data are listed in Table 6.

The cobalt complex exhibited two bands at 990 nm (10101 cm^{-1})], one of which refers to $^4T_1g_{(F)} \rightarrow ^4T_2g_{(F)}(v_1)$, transitions, [21,22], and the other at [653 nm (15313 cm^{-1})], which refers to $^4T_1g_{(F)} \rightarrow ^4T_1g_{(P)}$ (v_3) transitions [21,22].

Electronic spectrum of nickel (II) complex (C2)

The spectrum of the complex (C_2) as displayed in Figure 5 and the data are listed in Table 6.

The nickel complexes indicated two a bands at 901 nm (11098 cm^{-1}), this band refer to $^3A_2g_{(F)} \rightarrow ^3T_2g_{(F)}$ (v_1) transitions, and 635 nm (15748 cm^{-1}) which refer to $^3A_2g_{(F)} \rightarrow ^3T_1g_{(F)}$ (V_2) transitions [23,24].

Electronic spectrum of cupper (II) complex (C_3)

The spectrum of the complex (C_3) as depicted in Figure 6 and the data were listed in Table 6.

The copper complex exhibited two a bands at 910 nm (1098 cm^{-1}) this band assigned to $^2B_1g \rightarrow ^2A_1g$ (v_1) transition. The second band 705 nm (14184 cm^{-1}), this band refer to $^2B_1g \rightarrow ^2B_2g(v_2)$ transition [25,26].

Magnetic Susceptibility Studies

The magnetic susceptibility (μeff) was used to determine the structure of complexes. This measurement adds information about the strength of complex ligand fields and the number of unpaired electrons. For all complexes, the spin magnetic moment (s) $\mu eff_{(s)} = 2(s(s+1))^{1/2}$ was described by the spin quantum number (s) as follows: S = n/2 (n denotes the number of unpaired electrons). The magnetic moment of Cu (II) complex was 2.28 BM (Table 6), these values of μeff agreed with the distorted octahedral and indicated a paramagnetic character with a high spin orbital coupling and the magnetic moment of Ni(II) complex was 3.13. Co(II) complex 4.86 magnetic moments were paramagnetic and demonstrated octahedral geometries [27].

The conductivity measurements for complexes (C1-C3) in DMSO revealed that all complexes are electrolytes. The molar conductivity values in DMSO were 62.5, 64.4, and 77.2 μs/cm, indicating a 2:1 electrolyte of C1, C2, and C3 complexes [28].

Table 6: Electronic spectra, spectral parameters, molar conductance, magnetic susceptibility, and suggested geometry of metal complexes

Compound	Positions of the bands nm (cm^{-1})	Assignment	Molecular Conductivity (μs/cm) in Ethanol	μeff. (B.M)	Geometry suggestions
L_1	271(36900) 382 (26178)	(π-π*) (π-π*)	-----	-----	-----
C_1 Co	269(37174) 383(26109) V_2 653(15313) V_1 990(10101)	(π-π*) (π-π*) $^4T_1g_{(F)} \rightarrow ^4A_2g_{(F)}$ $^4T_1g_{(F)} \rightarrow ^4T_2g_{(F)}$	62.5	4.86	Octahedral
C_2 Ni	294(34013) 380(26315) $V_2$635(15748) $V_1$901(11098)	(π-π*) (π-π*) $^3A_2g_{(F)} \rightarrow ^3T_1g_{(F)}$ $^3A_2g_{(F)} \rightarrow ^3T_2g_{(F)}$	64.4	3.13	Octahedral
C_3 Cu	235(42553) 288(34722) 384(26041) V_2 705 (14184) V_1 910(10989)	(π-π*) (π-π*) (π-π*) $^2B_1g \rightarrow ^2B_2g$ $^2B_1g \rightarrow ^2A_1g$	77.2	2.28	distorted octahedral

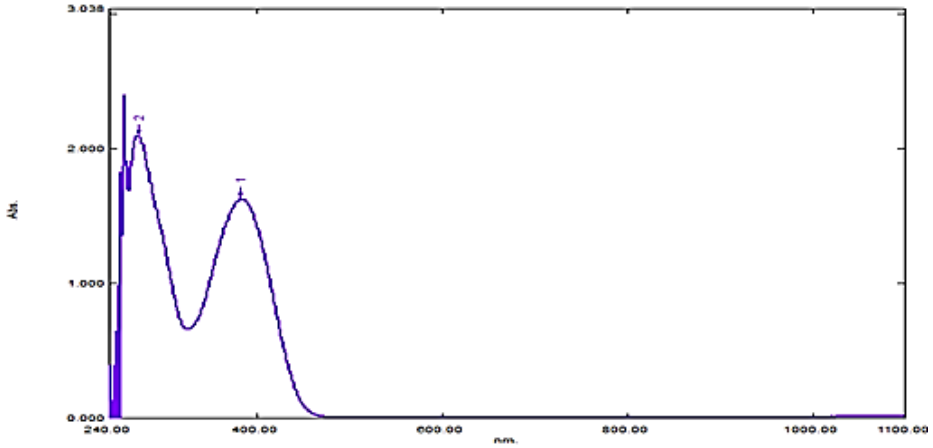

Figure 3: UV-Vis spectrum of the ligand

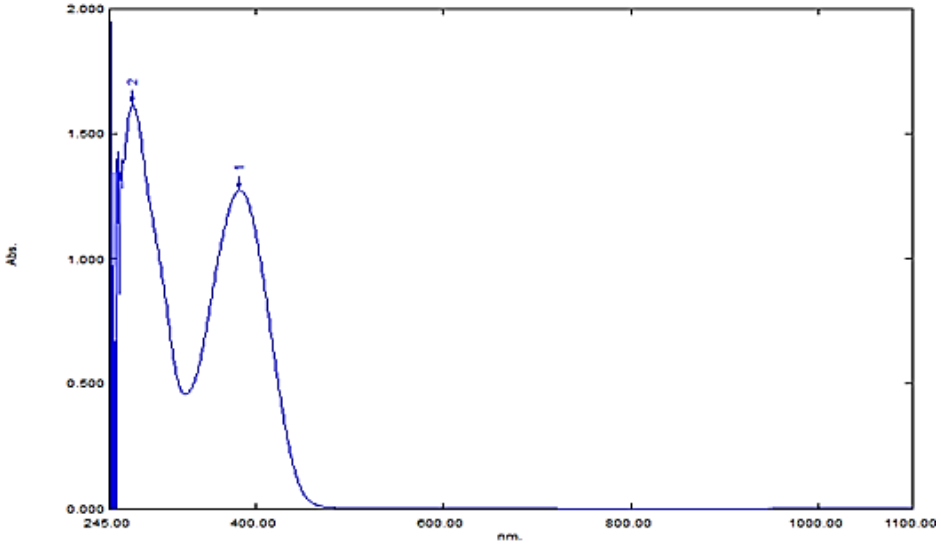

Figure 4: UV-Vis spectrum of the complex (C_1)

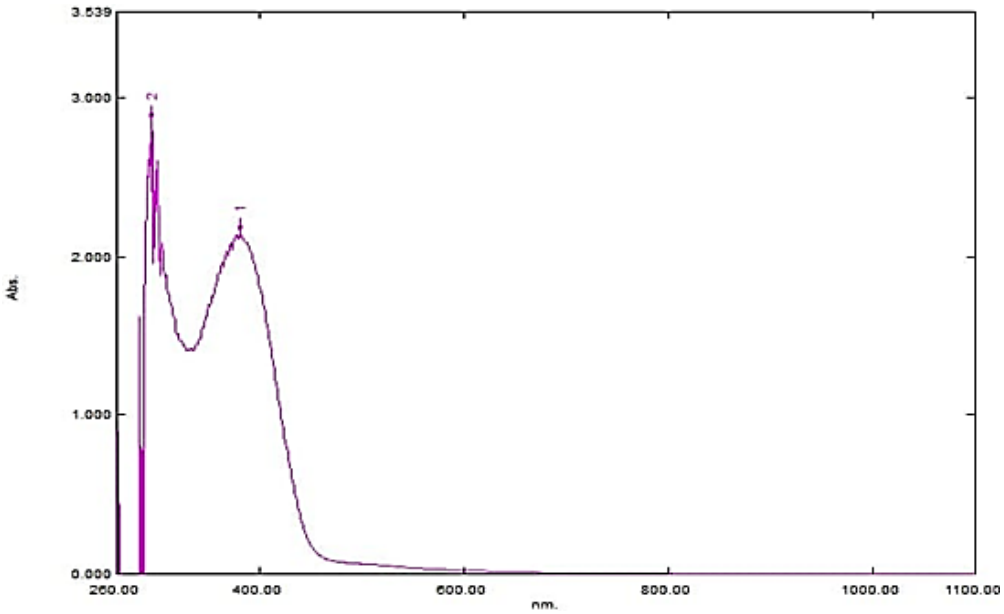

Figure 5: UV-Vis spectrum of the complex (C2)

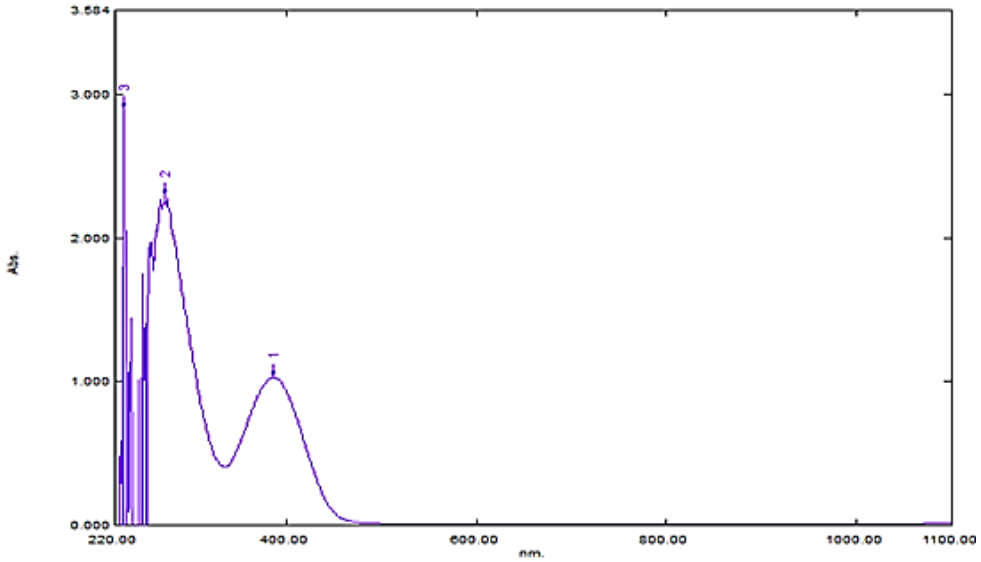

Figure 6: UV-Vis spectrum of the complex (C_3)

Biological Activity (Antimicrobial Activity)

The ligand and its metal complexes have anti-bacterial activity was investigated using the 10^{-3} M fusion process with DMSO as a solvent. The anti-bacterial and anti-fungal activity of the synthesized compounds was tested against *Staphylococcus aureus (G+), Klebsiella pneumoniae (G-),* and *rizopussporium.* The results indicate that sulfamethoxazole has less activity than tenoxicam and that ligand has more activity than both. The above results include both *Staphylococcus aurus (G+) and Klebsiella pneumonia (G-)*. In *Staphylococcus aurus*, the biological activity of ligand and its metal complex was as follows: LCo>L=LCu=LNi>tenoxicam >sulfamethoxazole at inhibition zone (22>21=21=21>15>14) mm and in *Klebsiella pneumonia*, ligand was more active than its complex, and the order was as follows: L>LCu> LNi> LCo. The results for anti-bacterial and anti-fungal dates were listed in Table 10 and the inhibition zones are displayed in Figures 7-9.

Table 7: The biological activity for studied compounds in (10^{-3} M)

Comp.	Staphylococcus aurus(G+)inhibiation zone diameter(mm)	Klebsiella pneumonia (G-)inhibiation zone diameter(mm)	Rizopussporium
DMSO	--	--	--
Sulfamethoxazole	14	11	16
tenoxicam	15	14	19
Ligand	21	25	12
LCo	22	21	13
LNi	21	22	19
LCu	21	24	12

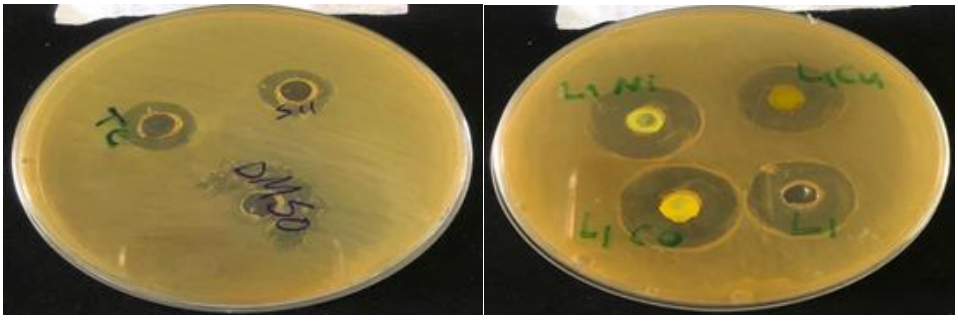

Figure 7: The inhibition zone for the ligand and its complexes, sulfametoxazole, tenoxicam, and DMSO against Staphylococcus aurus (G+)

Figure 8: The inhibition zone for the ligand and its complexes, sulfametoxazole, tenoxicam, and DMSO against Klebsiella pneumonia (G-)

Figure 9: The inhibition zone for the ligand and its complexes, sulfametoxazole, tenoxicam, and DMSO against Rizopussporium

Anticancer activity

The cytotoxic effect of the Sulfamethoxazole, Tenoxicam, and Ligand were examined with human hepatom cells (Hepg2) was carried out utilization of 3-(4,5-dimethylthiazol-2-yl)-2,5-diphenyltetrazolium bromide (MTT) assay method (Figures 10-12).

Table 8: Cytotoxicity effects of sulfamethoxazole against Hepg2 tumor cell line and normal cell line WRL-68

Cell line	Conc. µg/mL						IC50 µg/mI	P value
	400	200	100	50	25	12.5		
Hepg2	41.13±5.65	44.14±3.29	54.48±2.70	63.97±5.21	72.27±4.21	85.30±0.99	41.22	<0.0001
WRL	68.09±6.80	83.26±2.03	93.60±2.10	95.33±0.82	95.22±0.82	94.79±1.03	225.9	

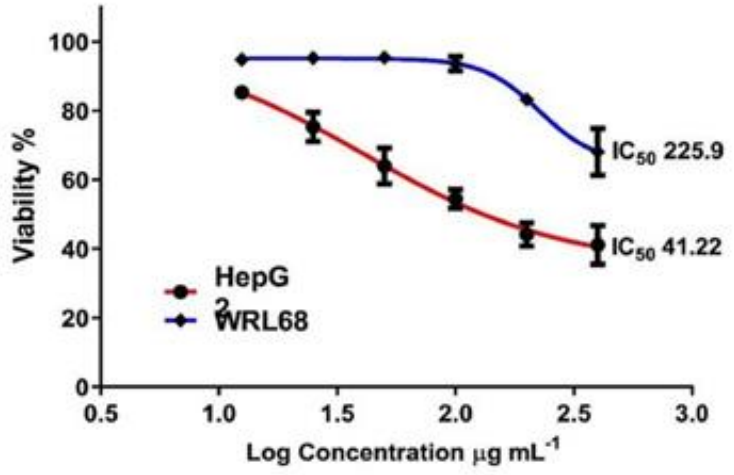

Figure 10: Cytotoxicity effect of sulfamethoxazole on Hepg2 cells after incubation for 24 hours at 37ºC (Log for the original concentration)

Table 9: Cytotoxicity effects of tenoxicam against Hepg2 tumor cell line and normal cell line WRL-68

Cell line	Conc. µg/mL						IC50 µg/ml	P value
	400	200	100	50	25	12.5		
Hepg2	48.61±5.92	61.19±2.59	76.35±3.48	90.36±1.64	96.95±1.75	96.03±3.08	133.8	<0.0001
WRL	68.09±6.80	83.26±2.03	93.60±2.10	95.33±0.82	95.22±0.82	94.79±1.03	318.9	

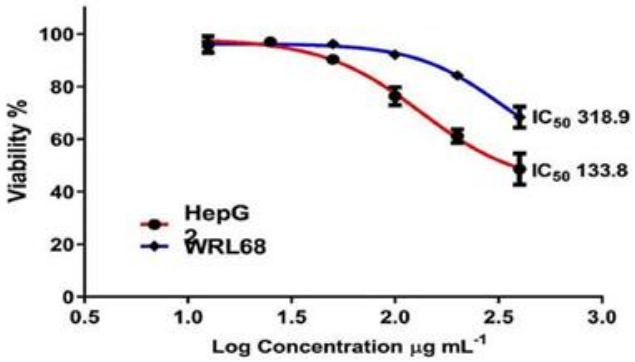

Figure 11: Cytotoxicity effect of tenoxicam on Hepg2 cells after incubation for 24 hours at 37ºC (Log for the original concentration)

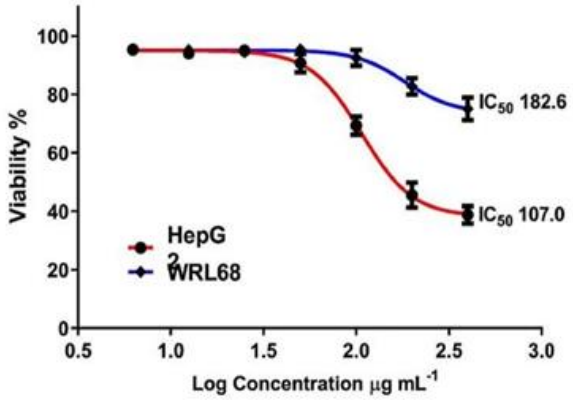

Figure 12: Cytotoxicity effect of Ligand on Hepg2 cells after incubation for 24 hours at 37ºC (Log for the original concentration)

From the result above indicate that ligand have higher killing effect comparison with sulfamethoxazole and tenoxicam.

Conclusion

The reaction of sulfamethoxazole and tenoxicam in a 1:1 mole ratio gave a new Schiff base ligand. Metal complexes with Co(II), Ni(II), and Cu (II) were synthesized in a 2:1 (L:M) mole ratio. All synthesized compounds were characterized, and the proposed structure was validated using spectral and physicochemical methods. The results revealed that all complexes have octahedral geometry and an electrolyte character. The biological results revealed that all of the synthesized compounds had excellent antimicrobial activity against bacteria *Staphylococcus aureus (G+), Klebsiella pneumoniae (G-)), and fungi Rizopussporium*. The synthesized ligand has anti-cancer activity**.**

Funding

This research did not receive any specific grant from funding agencies in the public, commercial, or not-for-profit sectors.

Authors' contributions

All authors contributed toward data analysis, drafting and revising the paper and agreed to responsible for all the aspects of this work.

Conflict of Interest

We have no conflicts of interest to disclose.

ORCID:
Amna Ahmed Neamah
https://www.orcid.org/0000-0003-4746-6679

References

[1]. Davies J., *J. Ind. Microbiol. Biotechnol.*, 2006, **33**:496 [Crossref], [Google Scholar], [Publisher]
[2]. Kotsiftopoulos C.H., *Arch. Med.*, 2017, **2**:36 [Google Scholar]
[3]. Ghernaout D., Elboughdiri N., *Appl. Eng.*, 2020, **4**:1 [Crossref], [Google Scholar], [Publisher]
[4]. García-Galán M.J., Díaz-Cruz M.S., Barceló D., *TrAC Trends Analyt. Chem.*, 2008, **27**:1008 [Crossref], [Google Scholar], [Publisher]
[5]. Bhattacharjee M.K., *Chem. Antibiotics Related Drugs,* 2016, 95 [Crossref], [Google Scholar], [Publisher]
[6]. Nesseem D.I., Eid S.F., El-Houseny S.S., *Life Sci.*, 2011, **89**:430 [Crossref], [Google Scholar], [Publisher]
[7]. Erbas M., Simsek T., Kiraz H.A., Sahin H., Toman H., *Rev. Bras. Anestesiol.*, 2015, **65**:333 [Crossref], [Google Scholar], [Publisher]
[8]. Adam A.M.A., *Appl. Organomet. Chem.*, 2018, **32**:e4055 [Crossref], [Google Scholar], [Publisher]
[9]. Masoud M.S., EAli A., Elasala G.S., Sakr S.F., Kolkaila S.A., *J. Chem. Pharm. Res.*, 2020, **12**:29 [Crossref], [Google Scholar], [Publisher]
[10]. Siraj I.T., Ado H.B., *ChemSearch J.*, 2021, **12**:27 [Crossref], [Google Scholar], [Publisher]
[11]. Gülcan M., Sönmez M., Berber İ., *Turk. J. Chem.*, 2012, **36**:189 [Crossref], [Google Scholar], [Publisher]
[12]. Ritika M.M., Barhate V.D., *Int. J. Chem. Tech. Res.*, 2014, **6**:1003 [Google Scholar
[13]. Chavda B.R., Socha B.N., Pandya S.B., Chaudhary K.P., Padariya T.J., Alalawy M.D., Patel M.K., Dubey R.P., Patel U.H., *J. Mol. Struct.*, 2021, **1228**:129777 [Crossref], [Google Scholar], [Publisher]
[14]. Zhou W., Moore D.E., *Int. J. Pharm.*, 1994, **110**:55 [Crossref], [Google Scholar], [Publisher]
[15]. Salem A.A., Mossa H.A., Barsoum B.N., *J. Pharm. Biomed. Anal.*, 2006, **41**:654 [Crossref], [Google Scholar], [Publisher]
[16]. Rostamizadeh S., Daneshfar Z., Moghimi H., *Eur. J. Med. Chem.*, 2019, **171**:364 [Crossref], [Google Scholar], [Publisher]
[17]. Kóczián K., Kökösi J., Mazák K., Noszál B., *Helv. Chim. Acta*, 2005, **88**:2355 [Crossref], [Google Scholar], [Publisher]
[18]. Defazio S., Cini R., *Polyhedron*, 2003, **22**:1355 [Crossref], [Google Scholar], [Publisher]
[19]. El-Gamel N.E.A., Gerlach D., *J. Coord. Chem.*, 2008, **61**:2246 [Crossref], [Google Scholar], [Publisher]
[20]. Qassim A.W., *Int. J. Adv. Sci. Tech. Res.*, 2015, **3**:135 [Google Scholar], [Publisher]
[21]. Al-Jebouri G.S., Noorikhaleel A.M., *Synthesis*, 2019, **12** [Crossref], [Google Scholar], [Publisher]
[22]. Mohamed G.G., El-Gamel N.E., Nour El-Dien F.A., *Synth. React. Inorg. Metal-Org. Chem.*, 2001, **31**:347 [Crossref], [Google Scholar], [Publisher]
[23]. Al-adely K.J., Dakhil H.K., Karam F.F., *J. Pure Sci.*, 2017, **16**:50 [Google Scholar], [Publisher]
[24]. Al-Adilee K.J., Abedalrazaq K.A., Al-Hamdiny Z.M., *Asian J. Chem.*, 2013, **25**:10475 [Crossref], [Google Scholar], [Publisher]
[25]. Khaleel A.M.N., Jaafar M.I., *Orient. J. Chem.*, 2017, **33**:2394 [Crossref], [Google Scholar], [Publisher]
[26]. Abdulghani A.J., Khaleel A.M.N., *Bioinorg. Chem. Appl.*, 2013, **2013** [Crossref], [Google Scholar], [Publisher]
[27]. Al-Abidy N.M.A., (Doctoral dissertation, University of Baghdad). 2006 [Google Scholar]
[28]. Yoshino T., *Surv. Geophys.*, 2010, **31**:163 [Crossref], [Google Scholar], [Publisher]

HOW TO CITE THIS ARTICLE
Amna Ahmed Neamah, Asmaa Mohammed Noori Khaleel. Synthesis of New Schiff Base from Antibiotics and Some of Its Metal Complexes with Study Some of Their Applications. *Chem. Methodol.*, 2022, 6(5) 372-384
https://doi.org/10.22034/CHEMM.2022.333061.1451
URL: http://www.chemmethod.com/article_147240.html